Simulation of connectivity of capillary porosity in hardening cement-based systems made of blended materials

Guang Ye, Klaas van Breugel

Microlab, Section of Materials and Environments, Faculty of Civil Engineering and Geosciences, Delft University of Technology, the Netherlands

In recent years, the durability of reinforced or prestressed concrete structures has become a main concern since engineers have to take into account the required service lifetime when selecting the concrete mixture and performing the structural design. A key parameter in durability predictions is the microstructure of the surface zone of concrete structures, i.e. the "covercrete", in particular the connectivity of the pores in the cement paste matrix because the easy of harmful substance, like chloride, enter to steel bar is determined by the connectivity of capillary pores in the concrete cover. In this paper, the connectivity of capillary pores in hardening cement-based system made of blended materials is studied numerically. The blended materials include blast furnace slag and limestone powder. In the numerical simulation, the hydration of the multi-components, i.e. cement particle and filler particle are considered. The stereological aspect, the interaction mechanism on both cement particle and filler particle, the basic rate equation and the influence factors are modeled. The simulated microstructure parameters, like capillary porosity and connectivity of capillary pores were analyzed based on the percolation theory. The simulation results were discussed and validated against experimental measurements. It is concluded that the connectivity of capillary pores can be manipulated by using different blended materials.

Key words: Blended cement, connectivity, numerical simulation

1   Introduction

Concrete is a heterogonous, multiphase materials consisting of solid phases (aggregates, calcium hydroxide and calcium silicate hydrates) and pore phases (capillary pores, gel pores and air voids). Theoretically, in the disordered multiphase media, like concrete, the disorder can be characterized by the degree of connectivity of the phases. In particular, the connectivity of pores at a predefined direction from one side to another side is defined as:

$$\text{Connectivity of pores } (\psi) = \frac{\text{Connected pore volume}}{\text{Total pore volume}} \tag{1}$$

When $\psi = 1$, means all pores are connected, $\psi = 0$, means that no pore path could go from one side to other side. The definition of connectivity of pores can also be applied to other phases in the porous media, like solid phase, capillary pores.

In physics, chemistry and materials science, percolation concerns the movement and filtering of fluids through porous materials [Stauffer, 1985] . The percolation threshold is the critical value of the occupation probability p, or more generally a critical surface for a group of parameters p_1, p_2, such that infinite connectivity (percolation) first occurs [Geoffrey, 1999]. In the cementitious system, the percolation threshold of capillary pores is the moment (degree of hydration or capillary porosity) when the capillary pores become discontinuous [Bentz and Garboczi, 1991]. It is accepted that in cementitious materials, the evolution of the connectivity of the solid is the basis for the evolution of the mechanical properties, whereas the de-percolation of the liquid phase, i.e. the formation of the pore structure, is the basis for the transport properties [Ye, 2005].

In recent years, use of supplementary cementitious materials, e.g. blast furnace slag and limestone powder as replacement of Portland cement have gained big attention. This is not only because of the low energy costs and the benefits on the environmental pollution but also the improvement of the concrete properties. Through the modification in concrete mixture, the connectivity of phases, the transport properties and mechanical properties can be changed and the durability of concrete is improved.

This research aims at a fundamental improvement of our understanding of the effect of the use of supplementary cementitious materials (active filler and inert filler) as replacements of cement and of the effect of these materials on the pore structures and on the connectivity of cement-based materials. In order to do so, the hydration and the microstructure development of blended cement was reviewed. The simulation models of blended cement are developed. Numerical experiments and application are presented as well. Completely new in this research is the idea to manipulate the connectivity (in view of decreasing the permeability) by changing the composition of the powder, i.e. by blending the cement with active or inert fillers. By performing these manipulations numerically and by taking into account a variety of relevant curing conditions, optimal powder and mixture compositions can be selected to meet required transport properties. In this way traditional experience-

based selection procedures can be replaced, or at least supported, by simulation-based procedures.

2 Hydration and microstructure development of blended cement

2.1 *Portland cement blended with Blast furnace cement*

The hydration of Portland cement blended with blast furnace slag (slag) is more complex than that of pure Portland cement since two components (cement and slag) hydrate simultaneously, and inter-react. When water is added in the Portland cement and slag mixture, Portland cement starts to hydrate immediately. Meanwhile, a small amount of slag reacts due to the presence of gypsum in cement. Then, the hydration of slag is greatly activated by alkalis and later by the Portlandite (CH). Similar to cement hydration, the hydration of slag also goes through three stages [Biernacki, Richardson, Stutzman and Bentz, 2002], namely: a nucleation period during which product growth is accelerating; a phase boundary controlled stage and a diffusion-controlled stage. From XRD study [Harrisson, Winter and Taylor, 1987], the hydration products of Portland cement blended with slag are essentially similar to those given by pure Portland cements hydration, i.e. calcite silicate hydrates (C-S-H), CH and Aft. New product, the hydrotalcite (M_5AH_{13}) is also found in the slag hydration. The stoichometry of slag hydration in Portland cement-slag system can be approximately written as [Mascolo and Marino 1980, Taylor 1997]:

$$C_{7.86}S_{7.38}M_{3.02}A + aCH + bH \rightarrow \iota C_nSH_m(M_xA)_y + \kappa M_5AH_{13} \qquad (2)$$

When 70% of cement is replaced by slag around 40-60% hydration products were identified as C-S-H by backscattering scanning electron microscopy image analysis [Ye, 2006]. XRD analysis shows that the CaO/Si ratio is lower in the C-S-H produced by slag-cement than produced by Portland cement paste [Taylor, 1997]. In the cement-slag hydration system, the quantities of CH are lower than those which would be given by the Portland cement constituent [Harrisson, Winter and Taylor, 1987]. The increasing amount of CH is slowed down when more cement is replaced by slag. CH initially increases then drops indicating that the CH not only acts as an activator for slag hydration, but also as a reactant.

Compared to Portland cement the hydration rate of slag is low. This is because the glassy surfaces of slag grains become coated with reaction products [Glaaser, 1982]. Experiments have shown that the reaction rate of slag decreases remarkingly with decreasing

water/powder ratio and with increasing amount of slag in the blends [Harrisson, Winter and Taylor, 1987].

The microstructure formation of slag in slag cement were observed to develop around slag grains, i.e., inner and out products. The most commonly observed type of microstructure is shown schematically in Figure 1, which is similar to the hydration of Portland cement.
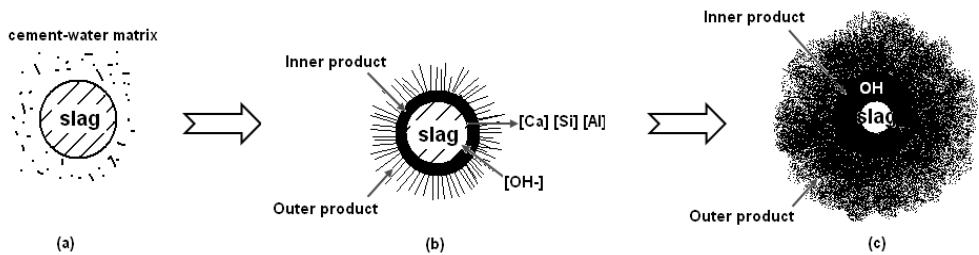

Figure 1: Schematic showing the progressive development of microstructure around a slag grain in cement paste (after [Glaaser, 1982])

The porosity and pore size distribution of hardening slag-cement paste are different from those of Portland cement [Zhou, Ye and Breugel, 2006]. In an early hydration stage, the porosity of slag-cement paste is higher. In a later stage due to reaction of slag the addition of slag leads to a fine pore system. The lower permeability value indicates that the pores in hardened slag-cement pastes are more discontinuous than that in Portland cement pastes [Zhou, Ye and Breugel, 2006].

2.2 *Portland cement blended with limestone powder*

The hydration of Portland cement blended with limestone powder was examined by isothermal conductive calorimeter [Ye, Liu, Poppe, De Schutter and van Breugel, 2007]. Figure 2 shows the heat release and the rate of heat release of two cement paste blended with limestone powder LP01 and LP02 compare with Portland cement paste CP. LP01 and LP02 made with same cement/powder ratio, 0.27 and difference water/cement ratio 0.41 and 0.48 respectively.

The results of the heat evolution show that the hydration is influenced by the presence of limestone filler. The cumulative heat release in cement paste containing limestone powder is higher and the rate of heat release is also higher than pure Portland cement paste. From Figure 2a, it can be concluded that the samples made with limestone filler (LP01 and LP02) show a higher heat release than traditional cement paste, especially in the first 24 hours.

The mixtures made with limestone filler show a shorter dormant stage and a more rapid heat release than mixtures without limestone filler. A maximum was found for both LP01 and LP02 mixtures at 12 hours. The rate of heat release curve (Figure 2b) indicates the rapid chemical reaction of cement blended with limestone powder in the early stage.
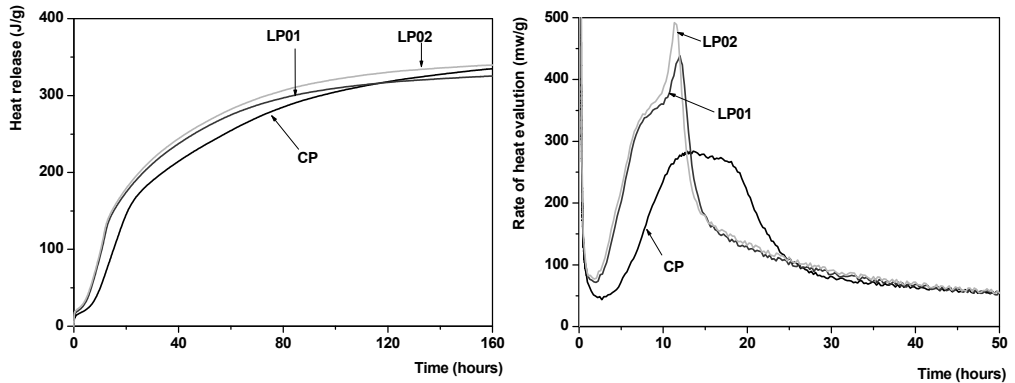

Figure 2: (a) Heat release of 3 different mixtures at 20 °C in the first 200 hours and (b). The rate of heat release of 3 different mixtures in the first 50 hours at 20 °C [Ye, Liu, Poppe, De Schutter and van Breugel, 2007].

To explain the shorter dormant stage and rapid heat release in the mixture with limestone filler two different hypotheses can be followed [Poppe, 2004]. The first hypothesis states that the limestone filler is inert and therefore does not take part in the reactions during the hydration. On the one hand, it will act as a nucleation core for the hydration of the C_3S and C_2S and shorten the dormant stage and fasten the hydration reactions. On the other hand the filler will activate reactions that are not or less prominently present in a traditional concrete without limestone filler which results in the third peak in the curve of the heat production rate.

The second hypothesis does not consider the limestone filler to be inert, but sees it as an active partner in the hydration reactions. The appearance of the extra hydration peak might then be explained by a conversion of ettringite to monocarbonate instead of monosulphate, which is a more stable compound and therefore results into more heat release, this with a peak at about 12 hours after the mixing of the components as a result. The development of the relative CH phases in LP is different from CP. The CH content in LP decreases till the curing age of 7 days and then increases. The fact that limestone

powder does not chemically react was confirmed both from thermal analysis and backscattering electron microscope (BSE) image analysis [Ye, Liu, Poppe, De Schutter and van Breugel, 2007].

The microstructure of the samples LP02 and CP at the age of 7 days examined by BSE are shown in Figure 3. It is found that the interface between limestone and hydrates is quite porous.
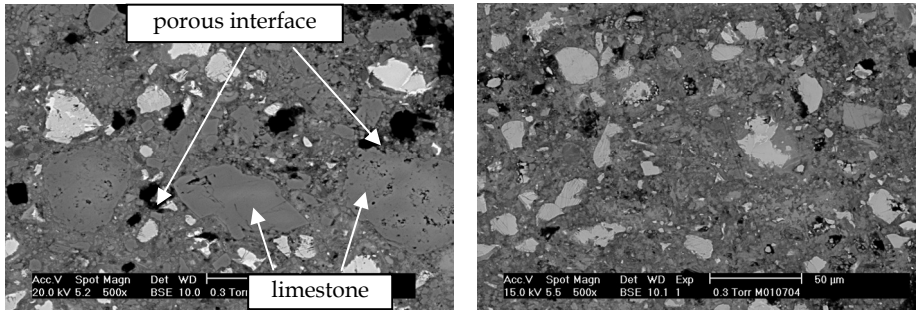

Figure 3: Comparison of BSE images for LP02 (left) and CP (right) at age of 7 days [Ye, Liu, Poppe, De Schutter and van Breugel, 2007]

From discussed above, it can be concluded that the presence of limestone powder in Portland cement promotes the chemical reaction by providing the nucleation site for the hydration of the C_3S and C_2S and thus increases the hydration rate at early stage. The mass of limestone powder does not change even at the hydration age of 28 days. Limestone powder can be treated as inert in the mixtures at the micro level. The interface between limestone and hydrates is porous.

3   Simulation of microstructure formation of blended cement

Simulation of the development of the microstructure of Portland cement containing filler is based on the 3D cement hydration computer model HYMOSTRUC3D [van Breugel 1997]. In order to simulate the hydration of cement containing filler powder, the characteristics of the paste is modified.

3.1   *Stereological aspects*

The cumulative particle size distributions of both cement and filler are described using the Rosin-Rammler function with constants b ($b > 0$) and n.

168

$$G_i(x) = 1 - \exp(-b_i x^{n_i}), \qquad \text{[g] } (x \text{ in } \mu m) \tag{3}$$

where, i is cement or filler. The maximum particle size x_{max} of cement or filler is defined as the particle with no more that 0.01 g oversize weight. The minimum particle size x_{min} of cement or filler is a realistic value, depending on the fineness of the cement or filler. The cement mass $W_{cem}(x)$ or filler mass $W_{filler}(x)$ of fraction F_x is obtained by differentiating Equation 3 with respect to x:

$$W_{cem}(x) = \gamma \times b_{cem} \times n_{cem} \times x^{n_{cem}-1} \times e^{-b_{cem} x^{n_{cem}}}, \qquad \text{[g]} \tag{4a}$$

$$W_{filler}(x) = \gamma \times b_{filler} \times n_{filler} \times x^{n_{filler}-1} \times e^{-b_{filler} x^{n_{filler}}}. \text{ [g]} \tag{4b}$$

For the volume V_x of all particles in fraction F_x, it holds that:

$$V_{cem}(x) = \frac{W_{cem}(x)}{\rho_{cem}}, \qquad \text{[cm}^3\text{]} \tag{5a}$$

$$V_{filler}(x) = \frac{W_{filler}(x)}{\rho_{filler}}. \qquad \text{[cm}^3\text{]} \tag{5b}$$

Where ρ_{cem} and ρ_{filler} are the specific mass of the cement and filler respectively. The number of particles N_x in fraction F_x is found by dividing the volume V_x of fraction F_x by the volume of a single particle v_x:

$$N_{cem,x} = \frac{V_{cem,x}}{v_{cev,x}} = \frac{\gamma \times b_{cem} \times n_{cem} \times x^{n_{cem}-1} \times e^{-b_{cem} x^{n_{cem}}}}{\frac{\pi \times x^3}{6} \times \rho_{cem} \times 10^{-12}}, \tag{6a}$$

$$N_{filler,x} = \frac{V_{filler,x}}{v_{filler,x}} = \frac{\gamma \times b_{filler} \times n_{filler} \times x^{n_{filler}-1} \times e^{-b_{filler} x^{n_{filler}}}}{\frac{\pi \times x^3}{6} \times \rho_{filler} \times 10^{-12}}. \tag{6b}$$

3.2 *Rate of penetration*

Figure 4 shows the mechanism of the interaction of cement particles and filler particles in cement-filler hydration system. The hydration of cement particles and slag particles both form inner and outer products. The small particles in the outer shell of the growing central particle create another additional outward growth of the outer shell. This additional growth results in encapsulation of more cement particles and hence in additional growth of the outer shell.

The incremental increase of the penetration depth $\Delta\delta_{in;x,j+1}$ of cement or filler particle x during a time increment $\Delta t_{j+1} = t_{j+1} - t_j$ equals:

$$\frac{\Delta\delta^i_{in;x,j+1}}{\Delta t_{j+1}} = K_i \times K_{filler} \times \Omega_1(\bullet) \times \Omega_2(\bullet) \times \Omega_3(\bullet) \times F_1(T) \times \left\{ F_2(\beta_2) \times \left[\frac{\delta_{tr}}{\delta} \right]^{\beta_1} \right\}^{\lambda}, \qquad (7)$$
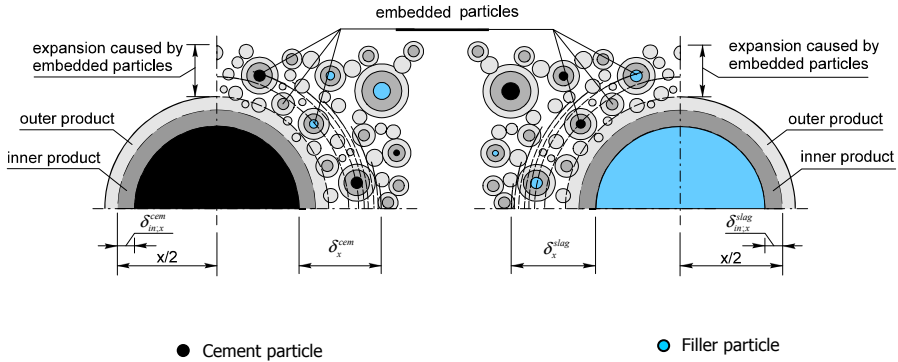
Figure 4: Particle interaction of cement particles and filler particles

where: K_i denotes the basic rate factor; for cement or slag and K_{filler} denotes the influence of amount of filler. $\Omega_1(x, a_{x,j})$ denotes the reduction factor accounting for water withdrawal effects as occurring for a particle with diameter x. $\Omega_2(a_j)$ and $\Omega_3(a_j)$ are the reduction factors accounting for water shortage in the pore system and for reduction of the amount of water in the hydrating mass. $F_1(\bullet)$ and $F_2(\bullet)$ are parameter taking into account the effect of the curing temperature on the rate of processes and the effect of curing temperature on morphology and formation of structure. λ denotes the factor depending on the rate-controlling mechanism, when $\lambda = 0$ for phase-boundary reaction and $\lambda = 1$ for diffusion-controlled reaction. β_1 and β_2 are constants. δ_{tr} is the transition thickness that determines

the change-over from a phase-boundary reaction into a diffusion-controlled reaction and δ is the total thickness of product layer [µm] of particle with diameter x at the end of time step Δt_j .

Details on determination of parameter listed in Eq. 7 were described in [van Breugel 1997]. New parameters, i.e., the basic rate factor K_i for slag and the influence factor K_{slag} will be discussed in the next paragrph.

The basic rate factor K_i for slag can be deduced from EDTA dissolution [Ye, 2007]. It was concluded that the hydration degree of slag is influenced by the amount of slag in slag cement. The higher proportion of slag results in lower hydration rate of slag due to the less CH produced from cement clinkers. The influence factor of cement hydration K_{slag} is also deduced from BSE image analysis combining with EDTA dissolution . From experiments, the hydration rate of Portland cement in slag-cement system goes faster than that in pure Portland cement paste. This can be attributed to the rich water (dilution effect) in the slag cement paste. In the blended cement paste, at same water/binder ratio, the rate of water consumption by slag is much slower. Consequently, the actual water/cement ratio in slag cement paste is higher than in pure Portland cement paste. According to Copeland and Kantro [1969], the alite and belite in a Portland cement hydrate more rapidly at high w/c at all ages from 1 day to 6.5 years. The rich water in slag cement paste certainly speeds up the hydration of cement clinker. This is also the case when Portland cement is blended with limestone powder. From discussion above, it is concluded that K_{slag} is a function of initial water/cement ratio and cement/powder ratio [Ye 2007]. For a mixture with w/c 0.40 and cement/powder ratio 0.50, the K_{slag} equals to 1.13.

Since limestone powder is considered an inert filler, which does not take part in the chemical reaction but accelerate the cement hydration in the early age, the basic rate factor K_i for limestone powder is 1. However, the hydration of Portland cement is speeded up by limestone powder acting as nucleation site for cement hydration products and by the dilution effect of limestone in the cement.

3.3   *Degree of hydration*

Similar to the original HYMOSTRUC [van Breugel, 1997] the degree of hydration of blended cement was considered on particle level, cell level and the overall degree of hydration. At the particle level, the increase of the degree of hydration $\Delta\alpha_{x,j}$ of cement particle or filler particle x that corresponds to an increase of the penetration depth $\Delta\delta_{x,j}$ during Δt_j follows from:

$$\Delta\alpha_{x,j}^{cem} = [1 - \frac{2\delta_{x,j-1}^{cem}}{x}]^3 - [1 - \frac{2(\delta_{x,j-1}^{cem} + \Delta\delta_{x,j})}{x}]^3, \tag{8a}$$

$$\Delta\alpha_{x,j}^{filler} = [1 - \frac{2\delta_{x,j-1}^{filler}}{x}]^3 - [1 - \frac{2(\delta_{x,j-1}^{filler} + \Delta\delta_{x,j})}{x}]^3. \tag{8b}$$

For the degree of hydration of particles x, i.e. fraction F_x, at time t_j is shows that:

$$\alpha_{x,j}^{cem} = \sum_{i=1}^{j} \Delta\alpha_{x,j}^{cem}, \tag{9a}$$

$$\alpha_{x,j}^{filler} = \sum_{i=1}^{j} \Delta\alpha_{x,j}^{filler}. \tag{9b}$$

At the cell level, the degree of hydration of a cell I_x follows from adding up the hydrated particle volume in fractions $F_z < F_x$ and dividing the sum by the original amount of particles:

$$\alpha_{\leq x,j}^{cem} = \frac{1}{(1 - m_{filler}) \times G_{cem}(x-1)} \sum_{z=x_{min}}^{x-1} \alpha_{z,j} \times (1 - m_{filler}) \times W_{cem}(z), \tag{10a}$$

$$\alpha_{\leq x,j}^{filler} = \frac{1}{m_{filler} \times G_{filler}(x-1)} \sum_{z=x_{min}}^{x-1} \alpha_{z,j} \times m_{filler} \times W_{filler}(z). \tag{10b}$$

The overall degree of the hydration can be computed as:

$$\alpha_j = \frac{1}{(1 - m_{filler}) \times G_{cem}(x_{max} - 1)} \sum_{z=x_{min}}^{x_{max}-1} \alpha_{z,j} \times (1 - m_{filler}) \times W_{cem}(z),$$
$$+ \frac{1}{m_{filler} \times G_{filler}(x-1)} \sum_{z=x_{min}}^{x-1} \alpha_{z,j} \times m_{filler} \times W_{filler}(z). \tag{11}$$

The volume of the outer product $V_{ou;x}^{cem}$ and $V_{ou;x}^{filler}$ for the cement particles and filler particle at a degree of hydration can be described as:

172

$$V_{ou;x}^{cem} = \left(v^{cem} - 1 \right) \alpha_j \times V_x^{cem},$$ (12a)

$$V_{ou;x}^{filler} = \left(v^{filler} - 1 \right) \alpha_j \times V_x^{filler}.$$ (12b)

where, α_j is overall degree of hydration according to Eq.11. v^{cem} and v^{filler} are the volume ratio of the reaction product and the dissolved material of cement or slag as described in [van Breugel, 1997]. These two parameters directly control the amount of hydration products produced by cement or filler at hydration degree α. In the case of limestone powder acting only as inert filler without participating in the chemical reactions, the v^{lim} should be equal to 1. Thus, there are no outer products formed around the limestone particles. Once the volume of outer products has been determined, the radius of the expanding central cement particle and the volume of expanded outer shell can be deduced.

4   Numerical experiments

The numerical experiments on the connectivity of capillary pores of hydrating cement pastes blended with blast furnace slag and limestone filler are studied in this section. The simulation takes into account the influence of the amount and the fineness of filler. The simulation results include the degree of hydration; the capillary porosity and the connectivity of capillary pore structure. The capillary pore phase and the connectivity of capillary pores were computed by using a serial section method combining an overlap algorithm [Ye 2003].

4.1   *Connectivity of Portland cement Blended with Blast Furnace Slag*

The simulation of slag cement was made by CEMI 42.5N blended with 0%, 30% and 50% slag; the w/binder ratio (w/b) was 0.40. The chemical composition of cement and slag used in the simulation were taken from [Zhou, Ye and Breugel, 2006].

Simulation starts by placing cement or cement and slag particles into a 100 μm^3 cube [Figure 6] following the particles size distribution (PSD) as showing in Figure 5. The simulated PSD were ultimately fitted with the experiments measured by laser diffraction particle size analyzer [Hackley, Lum, Gintautas and Ferraris, 2004].
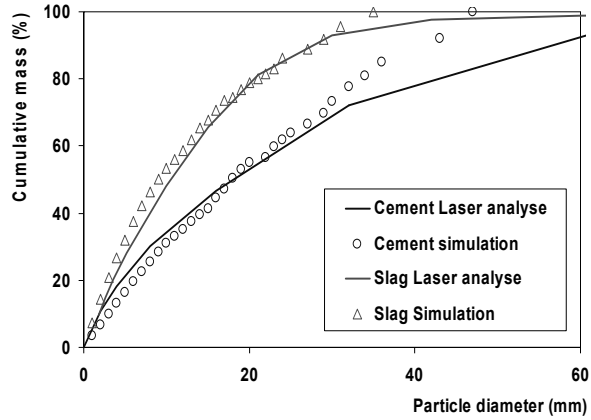
Figure 5: Simulation of PSD of CEMI 42.5N and blast furnace slag compared with the experiments measured by laser analyzer
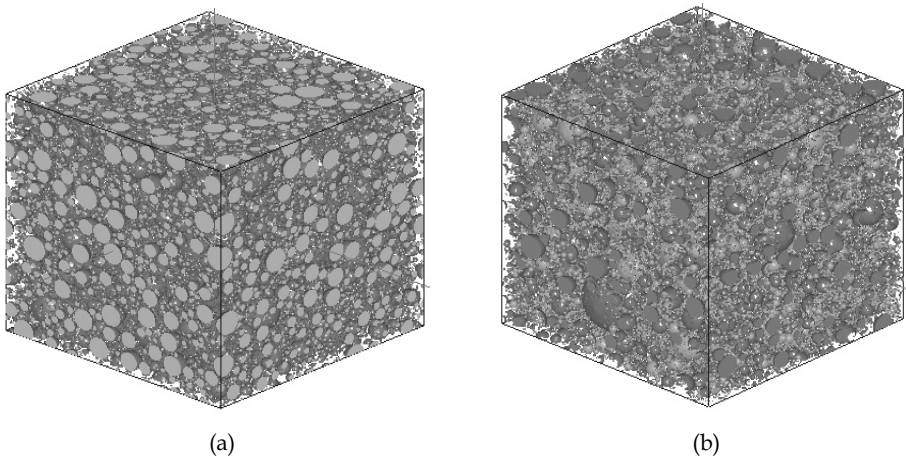

(a)	(b)

Figure 6: Initial particles distribution in the 100 m³ cube (a) cement paste, (b) 30% slag cement paste

4.1.1 Results and discussions

The degree of hydration of mixtures made with 30% and 50% slag were plotted in Figure 7 and compared with Portland cement paste. The simulated degree of hydration is in good agreement with experiments measured by BSE image analysis [Ye, 2007] and also compliance with the results reported by Lumley [Lumley, Gollop, Moir and Taylor, 1996]. It should be noted that the fully hydration of cement takes approximately 5 years,

however, 30% slag cement needs 23 years and 50% slag cement needs around 30 years reach to 100% hydration.
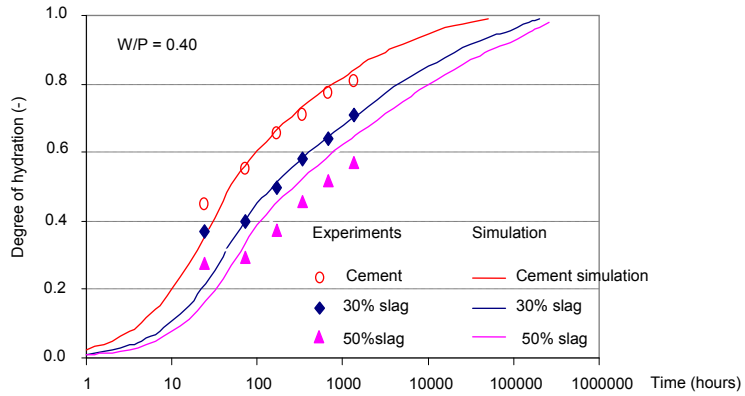
Figure 7: Comparison of degree of hydration by simulation and by experiments

Figure 8 show the connectivity of capillary porosity. It can be seen that at same capillary porosity, the connectivity of porosity is identical. This agrees with spherical based model where the particles are modeled as central growth. In Figure 8 (b), at 100% degree of hydration, there are still 82% capillary pores are connected in the cement paste and 60% of capillary pores are connected in the slag cement. No de-percolation of capillary porosity was found in both samples. The pore structure simulation do not agree with the experimental observation by Li and Roy [1986] and Osborne [1999], where a percolation of
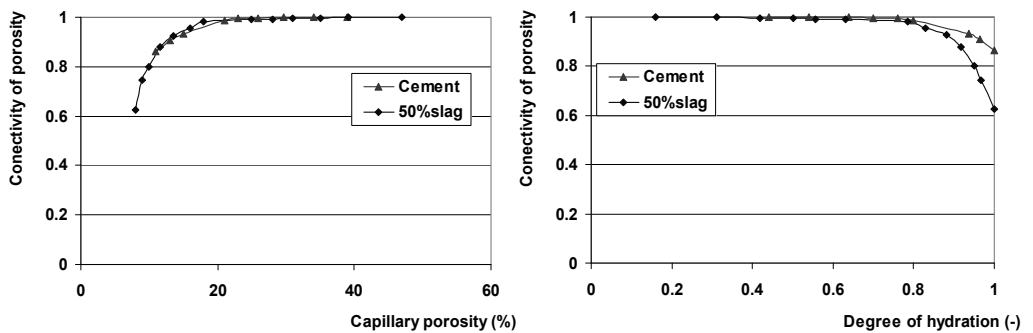
Figure 8: (a) The connectivity of capillary porosity as function of capillary porosity, (b) The connectivity of capillary porosity as function of hydration degree

175

capillary pore in slag cement paste was found at degree of hydration 0.85. This means that the present microstructure simulation of slag cement needs to improve. The modification of microstructure simulation of slag cement system is discussed in the next paragraph.

4.1.2 Modification of microstructural simulation in slag Cement system

Pore-space redistribution
In the slag cement paste, the hydration rate of cement is faster than that of slag due to the more water in the capillary pores. It was found that almost all initial cement particles have disappeared at around 1 year in slag cement paste with w/c ratio 0.40 [Ye, 2005]. However, when the cement clinkers have been used up, the pH value in the pore solution is still high enough for slag further hydration. This process can last for decades. During this period, the hydration products produced by slag slowly penetrate into the free pore space of cement paste as a consequence of pore-space redistribution [Glaaser, 1982]. The pore-space redistribution could block the capillary porosity and lead to a decrease in connectivity of pore structure.

In this part, the pore-space redistribution is considered in the simulation in order to improve the microstructure. This can be done by redistributing the hydration products of slag into the free pore space when the cement particles were fully hydrated. In the simulation the growth of outer shell of slag particle stops once the cement hydration reaches 100%. Instead, the volume of further hydration products of slag is converted into small pieces and redistributed in the free pore space. In this way, the capillary pores could be blocked and the pore system is becoming disconnected. At certain hydration degree, the total volume of out products of slag is converted into total volume of the redistributed hydration products. By assigning a diameter of free particles the total number of redistributed particles (called free particles) can be calculated. At an incremental hydration stage, the free particles further grow according to the total volume of outer products of slag. It is assumed that all free particles expand at same rate in the simulation.

Capillary Porosity and Connectivity of Pore Structure after Microstructural Modification
Example in Figure 9 schematically shows how the microstructure is modified by "free particles" redistribution.
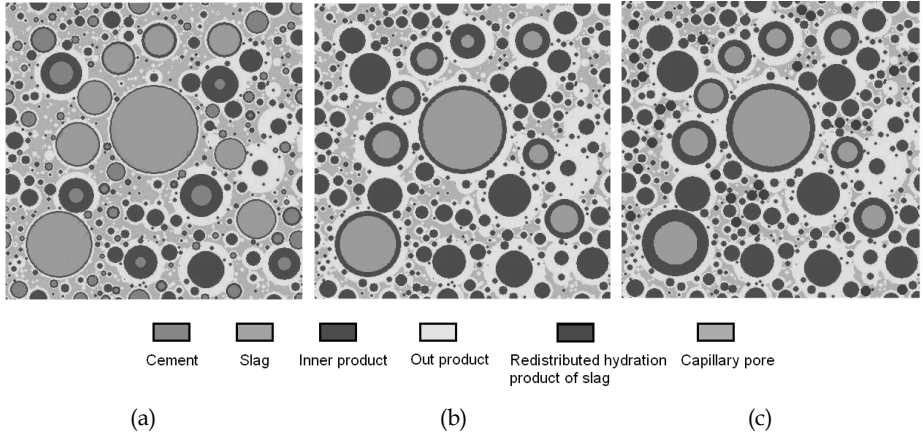
176

Figure 9: (a) Microstructure at overall degree of hydration 0.25, (b) Microstructure at overall degree of hydration 0.71, (c) Modified microstructure after free particles redistribution

In Figure 9a, at overall degree of hydration 0.25, both unhydrated cement and unhydrated slag are presented in the matrix. When the hydration degree reaches 0.71, the unhydrated cement particles have disappeared but a big amount of slag still remains in the matrix (Figure 9b). From this point on hydration products of slag penetrate through inner and outer products and precipitate in the free pore space (Figure 9c blue particles), resulting in a changed capillary pore structure.

By applying serial sectioning and overlap algorithm again on the modified microstructure, the capillary porosity and the connectivity of pore structure are computed (see Figure 10). After redistributing the slag hydration products in free pore space, the total porosity drops.
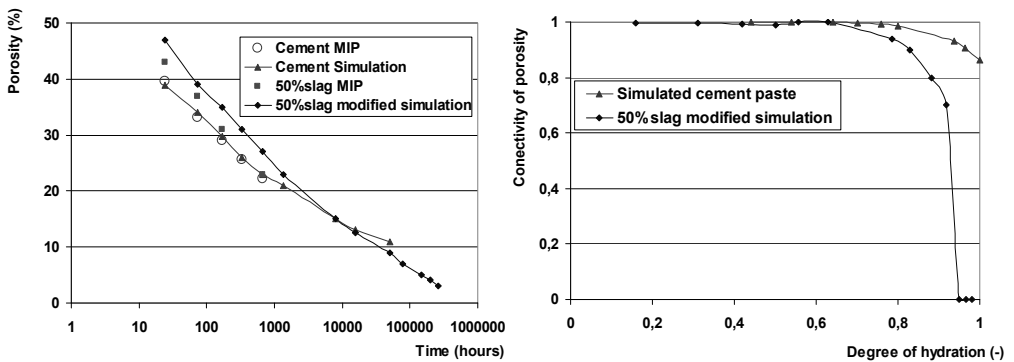
Figure 10: (a) Modified capillary porosity as function of time, (b) Connectivity of capillary porosity in modified microstructure as function of hydration degree
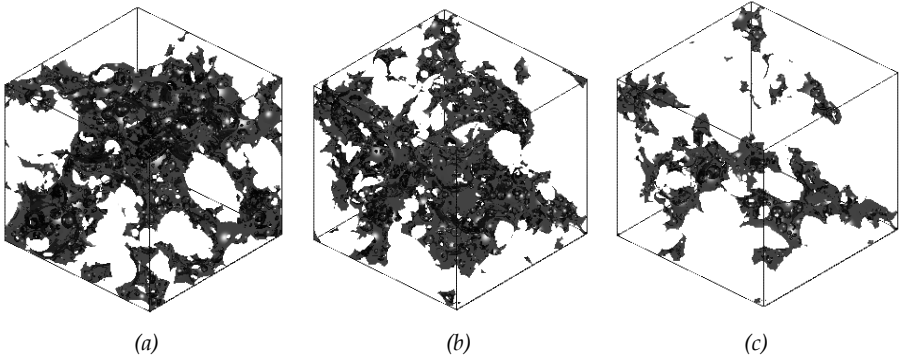
Figure 11: Capillary pore structures of the samples (a) Portland cement paste at degree of hydration 1, (b) 50% Slag cement paste at degree of hydration 1 before free particle redistribution (c) 50% Slag cement paste at degree of hydration 0.95 after free particles redistribution

The microstructure became denser. It is also found that a capillary porosity de-percolation occurs at degree of hydration 0.95 when the capillary porosity is 5.1% (see Figure10b). The modified capillary pore structure are in good agreement with experiments measured by mercury intrusion porosimetry method. Figure 11 show the visualized capillary pore structures. Apparently the capillary pore in 50% slag cement paste becomes disconnected after pore-space redistribution.

4.2   Connectivity of Capillary porosity of Cement Paste Blended with Limestone Powder

Input parameters

In the simulation, CEM I 52.5 was used. Two different water/powder (w/p) ratios 0.30 and 0.40; three different limestone filler contents, 10%, 20% and 30% by weight of cement; and three kinds of fineness (300, 400 and 500 m^3/kg) of limestone were considered. A continuous particle size distribution for both cement and limestone filler, with a particle size of minimum 1 μm and maximum 50 μm, was used. The size of all samples was 100×100×100 μm^3 in the simulation. The total amount of distributed cement and limestone filler particles in the cube are listed in Table 1. LP and CP indicate the cement paste with and without limestone filler.

The simulated 3D microstructures of CP01 and CL01 at the initial stage (a) and after 200 hours hydration (b) are shown in Figures 12. In Figure 12, the gray particles on the surface

Table 1 Initial number of particles in the calculation body of $100 \times 100 \times 100 \ \mu m^3$

Samples	W/P	Content Weight (%)	Fineness (m^3/kg)	Number of Cement Particles	Number of Limestone Particles
CP01	0.30	0	450	67487	0
LP01	0.40	30	400	45786	19658
LP02	0.30	30	400	51663	22184
LP03	0.40	10	400	53010	5835
LP04	0.40	50	400	36766	36463
LP05	0.40	30	500	45786	27695
LP06	0.40	30	600	45786	33349

are cement particles and the others are limestone powder. Comparing the pictures in Figure 12a, the limestone particles show no change during the hydration and are embedded in the hydrating cement particles (Figure 12b).

4.2.1 Connectivity of Capillary porosity

Figure 13 shows the influence of filler content on the connectivity of capillary porosity for the investigated samples. No de-percolation can be found from Figure 13, although the addition of limestone filler would decrease the porosity due to the filler effect. Figure 14 gives the connected pore fraction of samples with different limestone powder finenesses. The percolation is not affected by the fineness of limestone powder. The reason can be
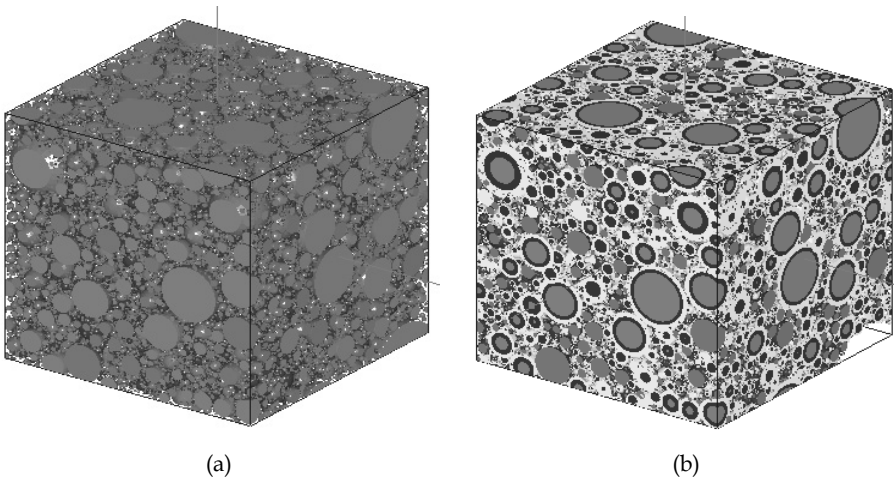

(a)   (b)

Figure 12: (a) Solid phase of paste LP01at initial stage and (b) solid phase of paste LP 01 after 200 hours of hydration

attributed to the fact that limestone powder acts as inert filler. The porous interface between limestone filler and hydration products lead to higher connectivity of capillary pores.

4.2.2 Discussion

Although experiments show that the limestone powder does not react chemically during hydration, its influence on the microstructure or other properties was not clear. Through numerical simulation of this study the effect of limestone filler can be studied more clearly. Based on the simulation, the influence of limestone powder can be classified into two periods along the hydration process. At the initial hydration stage, as limestone powders fill the space of hydrating cements, the microstructure of samples with addition of limestone filler is denser than those without limestone filler. This indicates that the samples with limestone filler should have good properties at initial age. With the process
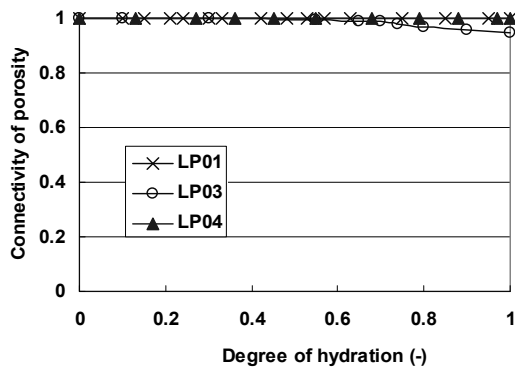

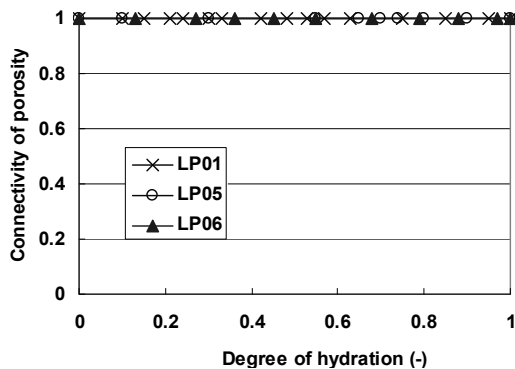*Figure 13: Influence of the filler content on the connectivity of capillary porosity*

Figure 14: Influence of fineness of limestone powder on the connectivity of capillary porosity

of hydration, the expanding cement particles connect and form a network, while at the same time, limestone powder particles do not expand during the whole process. Then the porosity for the samples without limestone addition becomes to be lower due to high amount of cement particle presented in the system

Furthermore, the addition of limestone filler could play a certain negative role as it could obstruct the expansion of hydrating cement. The interface between limestone filler and hydrates is quite porous. For the same water/powder ratio, cement paste samples show a de-percolation phenomenon at a certain degree of hydration, while the cement paste blended with limestone powder the capillary pores remain connected during the whole hydration process, which is shown in Figure 15. This is also demonstrated by the visualization of capillary pore structures of these two samples [Figure 16].
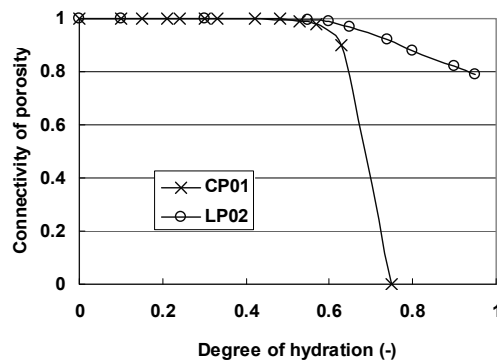

Figure 15: Comparison of cement paste made with and without limestone powder on connectivity of capillary porosity
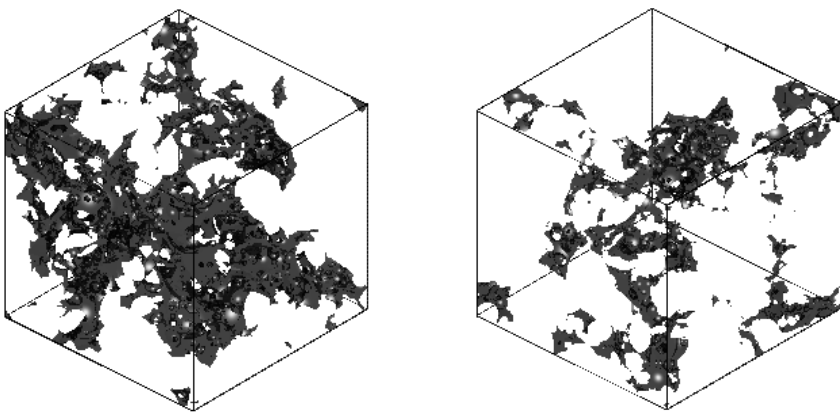

Figure 16: Capillary pore structures of the samples (a) LP02 at ultimate degree of hydration, (b) CP01 at ultimate degree of hydration

5   Conclusion

This paper present the simulation of connectivity of capillary pores of Portland cement paste blended with fillers. In the simulation, the hydration of the multi-components, i.e. cement particle and filer particle are considered. The stereological aspect, the interaction mechanism on cement particle and filler particle, the basic rate equation and the influence factors are modeled. Pore-space redistribution mechanism was applied in the simulation of the microstructure of slag cement paste.

From the simulation it can be concluded that the limestone powder acts as inert filler, its addition may provide a denser microstructure at the initial hydration stage, however, as the hydration proceeds, the cement paste with limestone powder shows looser microstructure because the limestone particles do not expand in the matrix as cement does. The de-percolation of capillary porosity was found in cement paste blended with slag; however the capillary porosity in cement paste blended with limestone filler will never reach de-percolation threshold.

It is concluded that the connectivity of capillary pore can be manipulated by using different blended materials.

Literature

Bentz, D. P., and Garboczi, E. J., "Percolation of Phases in a Three-Dimensional Cement Paste Microstructure Model," *Cement and Concrete Research*, V. 21, No. 2-3, 1991, pp. 325-344.

Biernacki, J. J., Richardson, J. M., Stutzman, P. E., and Bentz, D. P., 'Kinetics of Slag Hydration in the Presence of Calcium Hydroxide', *Journal of American Ceramic Society*, 85 (9) (2002) 2261-2267

Copeland, L. E., Kantro, D.L. in proceeding of the *5th International Symposium of cement chemistry* 2, (1969) 387.

Geoffrey, Grimmett. *Percolation* (2. ed). Springer Verlag, 1999.

Glaaser, F., 'Chemical, Mineralogical, and Microstructural Changes Occurring in Hydrated Slag-Cement Blends', *Materials Science of Concrete II.*

Harrisson, A.M., Winter, N.B. and Taylor, H.F.W., 'Microstructure and Microchemistry of Slag Cement Pastes,' *Mater. Res. Soc. Symp. Proc.*, 85, (1987) 213-222.

Hackley, V. A., Lum, L. S., Gintautas, V. and Ferraris, C. F., Particle Size Analysis by Laser Diffraction Spectrometry: Application to Cementitious Powders, *NISTIR 7097*; March 2004.

Li, Shiqun. and Roy, D. M. 'Investigation of relations between porosity, pore structure, and C1− diffusion of fly ash and blended cement pastes,' *Cement and Concrete Research*, 16 (5) (1986) 749-759.

Lumley, J. S., Gollop,R. S., Moir, G. K. and Taylor, H. F. W. 'Degrees of reaction of the slag in some blends with Portland cements', *Cement and Concrete Research* 26 (1) (1996) 139-151.

Mascolo, G. and Marino, O., 'A New Synthesis and Characterization of Magnesium-Aluminum Hydroxides,' *Mineral*. Mag., 43 (1980) 619–621.

Osborne, G. J., 'Durability of Portland blast-furnace slag cement concrete, *Cement and Concrete Composites*, 21 (1) 1999 11-21.

Poppe, A.-M. '*Influence of fillers on hydration and properties of self-compacting concrete*', PhD thesis (in Dutch), Ghent University, 2004

Stauffer, D., *Introduction to Percolation Theory*, Taylor and Francis, London, 1985, pp. 1-72.

Taylor, H. F. W., (1997) *Cement Chemistry*, 2nd Ed. Thomas Telford Publishing, London. U.K.

van Breugel, K., *Simulation of Hydration and formation of structure in hardening cement-based materials*, Second Edition, PhD thesis, Delft University of Technology, Delft, 1997

Ye, G. '*The microstructure and permeability of cementitious materials*', PhD thesis, Delft University of Technology, Delft, 2003.

Ye, G., "Percolation of capillary pores in hardening cement pastes" *Cement and Concrete Research* 35 (1), 167-176, 2005.

Ye, G., 'Numerical simulation of connectivity of individual phases in hardening cement-based systems made of blended cement with and without admixtures', *VENI* report, the Netherlands, Jan, 2007.

Ye, G. Liu, X. Poppe, A.M. De Schutter, G and van Breugel, K. (2007) Numerical Simulation of the Hydration Process and the Development of Microstructure of Self-Compacting Cement Paste Containing Limestone as Filler, *Materials and Structures / Matériaux et Construction*, 40 (9) 865-875.

Zhou, J, Ye, G and Breugel, K van. 'Hydration process and pore structure of Portland cement paste blended with blast furnace slag'. In S Tongbo, S Rongxi, Z Wensheng, &

Wensheng (Eds.), *Cement & Concrete, contribute to global sustainability*. Beijing: Foreign Languages Press (2006) 417-424.